

## ANALYSIS OF THE CONVECTIVE HEAT TRANSFER OF A FLUID FLOW OVER AN IMMERSED AXI-SYMMETRICAL BODY WITH CURVED SURFACES

**M. N. Kinyanjui, D. G. Kioi and J. K. Kwanza**

*Department of Pure and Applied Mathematics, Jomo Kenyatta University of Agriculture and Technology, Nairobi, Kenya*

*E-mail: mathewkiny@yahoo.com*

### **Abstract**

Convective heat transfer in a homogeneous fluid flow Reynolds number of order less than 2000 over an immersed axi-symmetrical body with curved surfaces has been investigated. The fluid flow in consideration was unsteady and of constant density. This study analysed the extent to which convective heat transfer has on drag and lift on bodies submerged in fluid. The different temperature profiles which were as a result of temperature gradients, caused the convective heat transfer. These different temperature profiles were brought about by frictional forces on and within the surface of the body when fluid flowed over it. Velocity variations were also determined and were used to evaluate these temperature profiles. To obtain these profiles, various flow parameters were varied in the equations governing the fluid flow. These equations were non-linear and there exists no analytical method of solving them, hence a suitable numerical method in this case finite difference method was used. Results of the velocity variations and temperature variations were obtained followed by graphical representation of the results. It was however noted that when the Reynolds number was increased, the heat dissipation also increased, when the curvature of the surface was increased, the dissipation also increased. These results have major application in designing devices requiring high manoeuvrability and less resistance to the motion e.g. aerofoil, spray atomizers and cooling fans.

**Key words:** Homogeneous, convective heat transfer, axi-symmetrical

**Nomenclature**

<b>Symbol</b>	<b>Meaning</b>
$C_p$	Specific heat at constant pressure. $\text{Jkg}^{-1} \text{K}^{-1}$
$L$	Reference length ,M
$m$	Real number
$P$	Pressure, Pa
$E_c$	Eckert number
$Pr$	Prandtl number
$Pe$	Peclet number
$Re$	Reynolds number
$Q$	Quantity of heat added to the system, Joules (J)
$\dot{q}$	Heat generated in the boundary layer, Joules
$T$	Temperature, K
$T_s$	Temperature of the body's surface, K
$T_\infty$	Free stream temperature, K
$h$	heat transfer coefficient. $h=q_w(T_w-T_\infty)$ , $\text{W/m}^2\text{K}$
$U$	Outer flow fluid velocity in the x-direction, $\text{ms}^{-1}$
$V$	Reference fluid velocity in the y-direction, $\text{ms}^{-1}$
$F_x, F_y$	Body forces, Newtons along the x and y directions respectively
$x, y, z$	Cartesian co-ordinates
$i, j, k$	Unit vectors in the x, y and z directions respectively
$\frac{D}{Dt}$	Material derivative $\left( = \frac{\partial}{\partial t} + u \frac{\partial}{\partial x} + v \frac{\partial}{\partial y} + w \frac{\partial}{\partial z} \right)$
$\vec{\nabla}$	Gradient operator $\left( i \frac{\partial}{\partial x} + j \frac{\partial}{\partial y} + k \frac{\partial}{\partial z} \right)$
$\nabla^2$	Laplacian operator $\left( \frac{\partial^2}{\partial x^2} + \frac{\partial^2}{\partial y^2} + \frac{\partial^2}{\partial z^2} \right)$

$\vartheta$	Kinematic viscosity, $\text{m}^2\text{s}^{-1}$ $\vartheta = \frac{\mu}{\rho}$
$\mu$	Absolute viscosity (dynamic viscosity coefficient), kg/ms
$\rho$	Fluid density, $\text{kgm}^{-3}$
$\varphi$	Viscous dissipation function
$\delta$	Boundary layer thickness, m
$\sigma_{i,j}$	Normal stresses, $\text{Nm}^{-2}$
$\tau_{i,j}$	Shear stresses, $\text{Nm}^{-2}$

## 1.0 Introduction

The theory of convective heat transfer strongly emerged in 20<sup>th</sup> century. By its nature, convective energy transfer is closely related to fluid particles motion and therefore is a fundamental part of fluid mechanics study. Advancement in research in fluid mechanics (particularly hydrodynamics of non-Newtonian, electric current-conducting and magnetic media, supersonic and hypersonic gas dynamics, dynamics of plasma, fine molecular and heterogeneous flows, the hydro and gas dynamics effects during heat transformation) have greatly affected the theory of heat and mass transfer in moving media e.g. air, water and oil. The relationship between the intensities of turbulent momentum and heat transfer process is one of the subtle problems of heat transfer theory

A number of experimental and numerical studies of convective heat transfer over curved surfaces have been done. The measurement and prediction of the rate of heat transfer for a two dimensional boundary layer on a concave surface have been presented by Mayle *et al.* (1979). It was established that the heat transfer on the convex surface was less than that of a flat surface having the same free stream, Reynolds number and turbulence. Concave surface heat transfer was augmented when compared to the flat surface. In the turbo machinery applications; a variations in the rate of heat transfer due to a small flow disturbance can lead to an increase in the thermal stress and decrease the effective working life span of such a component. On a highly curved wall, the change in heat transfer rate is mainly due to an increase or decrease of the turbulent mixing by effect of streamline curvature. It has been indicated in Von Karman's stability argument (1934) that the convex wall has a stabilizing effect on the fluid particles, while concave wall has a de-stabilizing effect with reference to a flat plate.

There have been many previous investigation of flow and heat transfer on flat plate boundary layers with pressure gradients. Fukagata *et al* (2002) were concerned with transition to turbulent flow and the Reynolds stress distribution. Mei *et al* (1999) and Bouzidi *et al* (2001) proposed some other boundary treatment

methods. In all those methods, the boundary conditions were treated separately for some specific steps when some variations occurs in the specified steps while dealing with curved boundaries, an abrupt change in the single particle mass distribution was caused. Filippova and Hanel (1998) developed a curved boundary treatment using Taylor's series expansion in both space and time for single particle distribution near the wall. This boundary condition satisfies the no-slip condition to the second order in a space step and preserves the geometrical integrity of the wall boundary.

Barenblatt *et al.* (2002), in their study on the model of the turbulent boundary layer with non- zero pressure gradient observed that the turbulent boundary layer at large Reynolds number consist of two separate layers upon which the structure of the vortex fields is different, although both exhibit similar characteristics. In the first layer, vertical structure is common to all developed bounded shear flows and the mean flows. The influence of viscosity is transmitted to the main body of flow via streaks separating the viscous sub layer. The second layer occupies the remaining part of the intermediate region of the boundary layer. The upper boundary of the boundary layer is covered with statistical regularity by large scale "humps" and the upper layer is influenced by the external flow via the pressure drag of these humps as well as by the shear stress. In their earlier works it is shown that the mean velocity profile is affected by the intermittency of the turbulence and as the humps affects intermittency, the two seeking regions are visible. On the basis of these considerations, the effective  $Re$ , which determines the flow structure in the first layer (and is affected in turn by the viscous sub layer), was identified as one set of such parameters. The other parameters that influence the flow in the upper layer include pressure gradient,  $\frac{\partial P}{\partial x}$ ; dynamic (friction) viscosity,  $\mu$ ; velocity,  $u$ ; fluid's kinematic viscosity,  $\nu$  and density,  $\rho$ . Khoshevis *et al* (2007) investigated the effects of the concave curvature on turbulent flows using numerical solutions of boundary layer equations on concave surfaces. It was evident that turbulent intensities and turbulent shear stresses are increased on concave walls compared to flat plates under same conditions and they concluded that for the boundary layer on concave surfaces, the destabilizing effects lead to increased turbulent momentum exchange between the fluid particles similar to the way concave curvature causes flows to be destabilized. In this study, a body having both convex and concave surfaces was considered and the effects of these surfaces on the dissipation of heat investigated.

## 2.0 Mathematical Formulation

The fluid in consideration was Newtonian and had constant density whose Reynolds number was less than 2000. The equations governing the flow were reduced from the general ones through assumptions mentioned above and most of the analysis done was in the boundary layer region. . The equations governing the fluid flow in tensor form were given as;

$$\frac{\partial u_i}{\partial x_i} = 0 \dots \dots \dots (1)$$

$$\frac{\partial u_i}{\partial t} + u_j \frac{\partial u_i}{\partial x_j} = -\frac{1}{\rho} \frac{\partial P}{\partial x_i} + F_i + \nu \nabla^2 u_i \dots \dots \dots (2)$$

$$\rho c_v \frac{DQ}{Dt} = \frac{\partial}{\partial x_i} \left( k \frac{\partial Q}{\partial x_i} \right) + \frac{1}{2} \mu \left( \frac{\partial u_j}{\partial x_i} + \frac{\partial u_i}{\partial x_j} \right)^2 \dots \dots \dots (3)$$

Equations 1, 2 and 3 represent continuity, momentum and energy conservation equations respectively. These equations for a curved surface reduced to

$$\frac{\partial u}{\partial t} = P_t + \nu \frac{\partial^2 u}{\partial y^2} + F_x \dots \dots \dots (4)$$

$$c_p \rho \frac{\partial T}{\partial t} = k \frac{\partial^2 T}{\partial y^2} + \mu \left( \frac{\partial u}{\partial y} \right)^2 + \dot{q} \dots \dots \dots (5)$$

The study of the analogy between buoyancy and curvature effects to the boundary layer flow were first studied by Prandtl(1904). From Khosevis *et al* (2007), convex curvature boundary layer exert a stabilizing effect while concave exhibit unstabilizing effect. Prandtl proposed that to account for the curvature effect, the length of the body's surface is multiplied by a dimensionless factor

$$f = 1 - \frac{1}{4} \frac{k_r u}{\left( \frac{\partial u}{\partial y} \right)} \dots \dots \dots (6)$$

This was supported by experiments by Wilken and Schmidbauer (1966). From their experiments they deduced boundary layer equations for curved surface as

$$\frac{k_r u^2}{h_1} = \frac{1}{\rho} \frac{\partial P}{\partial y} \dots \dots \dots (7)$$

Where  $k_r$  and  $h_1$  are curvature parameters which are defined as;

$$k_r(x) = -\frac{1}{r(x)} \dots \dots \dots (8)$$

$$h_1 = 1 + k_r y \dots \dots \dots (9)$$

Where,  $r(x)$  is the radius of the curved surface. Equations 1, 2 and 3 yielded

$$\frac{\partial u}{\partial t} = P_t + \nu \frac{\partial^2 u}{\partial y^2} + k_r u^2 \dots \dots \dots (10)$$

$$c_p \rho \frac{\partial T}{\partial t} = k \frac{\partial^2 T}{\partial y^2} + \mu \left( \frac{\partial u}{\partial y} \right)^2 + k \left( 1 - \frac{1}{4} \frac{k_r u}{\left( \frac{\partial u}{\partial y} \right)} \right) A (T_\infty - T_s) \dots \dots \dots (11)$$

The boundary conditions for the fluid flow over an axi-symmetrical body with curved surfaces, taking into consideration the no-slip condition and negligibility of the effects of viscous forces in the free stream region. The initial conditions were obtained by assuming the fluids velocity was zero at the leading edge. Equations 10 and 11 were solved subject to the following initial and boundary conditions respectively;

$$\begin{aligned} u(t, 0) &= 0 \\ u(t, \infty) &= u_0 \\ u(0, y) &= 0 \end{aligned}$$

and

$$\begin{aligned} T(t, 0) &= T_s \\ T(t, \infty) &= T_\infty \\ T(0, y) &= 0 \end{aligned}$$

On non-dimensionalising equation 10 and 11 and the initial and boundary conditions using the transformations:

$$\begin{aligned} x = x^* L, \quad y = y^* L, \quad u = u^* V, \quad v = v^* V, \quad P = P^* P, \quad T^* = \frac{T - T_s}{T_\infty - T_s}, \\ t^* = \frac{tV}{L} \quad \text{or} \quad t = \frac{t^* L}{V} \end{aligned}$$

Equations 10 and 11 together with dimensionless numbers yielded

$$\frac{\partial u^*}{\partial t^*} = \frac{PL}{V^2} P_t^* + \frac{1}{Re} \frac{\partial^2 u^*}{\partial y^{*2}} + k_r L U^{*2} \dots \dots \dots (12)$$

Subject to

$$\begin{aligned} u^*(t^*, 0) &= 0 \\ u^*(t^*, \infty) &= 1 \\ u^*(0, y^*) &= 0 \end{aligned}$$

and

$$\frac{\partial T^*}{\partial t^*} = \frac{1}{Pe} \frac{\partial^2 T^*}{\partial y^{*2}} + \frac{Ec}{Re} \left( \frac{\partial u^*}{\partial y^*} \right)^2 + \frac{L^2 A}{Pe} \left( 1 - \frac{k_r u^* L}{4 \left( \frac{\partial u^*}{\partial y^*} \right)} \right) \dots \dots \dots (13)$$

Subject to;

$$T^*(t^*, 0) = 0$$

$$T^*(t^*, \infty) = 1$$

$$T^*(0, y^*) = 0$$

**2.1 Method of Solution**

Equations 12 and 13 were non-linear time dependent equations and to solve them an appropriate numerical method was required, in this case finite difference method was used. The finite difference grid was used to calculate the values at the mesh point and each nodal point was identified by a double index (i, j). i was set to start at 0 to 40 in the computational forward difference grid while j was also set to start from 0 to 40 in the grid. Equation 12 and 13 were rewritten in forward difference and in conjunction with Crank Nicolson approximation as;

$$u_{i+1,j}^* = \frac{\left[ u_{i,j}^* + \frac{\Delta t PL}{V^2} P_{t_i}^* + \frac{\Delta t}{Re} \left[ \frac{u_{i+1,j+1}^* + u_{i+1,j-1}^* + u_{i,j+1}^* - 2u_{i,j}^* + u_{i,j-1}^*}{2(\Delta y)^2} \right] + \Delta t k_r L u_{i,j}^{*2} \right]}{\left( 1 + \frac{\Delta t}{Re(\Delta y)^2} \right)} \quad (14)$$

Subject to;

$$u^*(40,0) = 0$$

$$u^*(40,40) = 1$$

$$u^*(0,40) = 0$$

and

$$\begin{aligned}
T_{i+1,j}^* = & \left( T_{i,j}^* + \frac{\Delta t}{Pe} \left[ \frac{T_{i+1,j+1}^* + T_{i+1,j-1}^* + T_{i,j+1}^* - 2T_{i,j}^* + T_{i,j-1}^*}{2(\Delta y)^2} \right] \right. \\
& + \frac{\Delta t Ec}{Re} \left[ \frac{u_{i+1,j+1}^* - u_{i+1,j}^* + u_{i,j+1}^* - u_{i,j}^*}{2\Delta y} \right]^2 + \frac{\Delta t L^2 A}{Pe} \\
& \left. - \frac{\Delta t AL^3 k_r u_{i,j}^*}{4Pe \left[ \frac{u_{i+1,j+1}^* - u_{i+1,j}^* + u_{i,j+1}^* - u_{i,j}^*}{2\Delta y} \right]} \right) \\
& \div \left( 1 + \frac{\Delta t}{Pe(\Delta y)^2} \right) \dots \dots \dots (15)
\end{aligned}$$

Subject to;

$$T^*(40,0) = 0$$

$$T^*(40,40) = 1$$

$$T^*(0,40) = 0$$

### 3.0 Results and Discussion

On using a computer program so developed for this specific research problem, the results were obtained by varying Reynolds number  $Re$ , Eckert number  $Ec$ , Peclet number and surface curvature,  $Kr$ .

From Figure 1, we noted that:

(i) When Reynolds number was increased from 5 to 10, we noted that from curve-ii, the free stream velocity of the fluid particles reduced from 2.50423866 m/s to 0.937234433 m/s.

This was because when  $Re$  was increased, inertia forces increased and these forces tend to oppose bodies from accelerating hence reduced velocities.

(ii) When the radius of curvature,  $Kr$  was increased from 0.5 to 1, we obtained curve-iii where the free stream velocity of the fluid particles increased from 2.50423866m/s to 3.904712m/s.

This was because when the curvature was increased, this led to increase in the velocity gradient hence increased velocities. If the curvature of a particular body is increased the velocity gradient also increased and when the curvature was reduced the velocity gradient reduced.



From Figure 2 we note that:

(i) When Re was increased from 5 to 10, from curve-ii we noted that the heat dissipated in the boundary layer reduced from 0.579673 K to 0.0559 K.

This was because when the value of Re was small the viscous forces dominated over the inertia forces and if this was the case, large viscous forces resulted to increased friction between the surface of the body and fluid which also brought about increased dissipation of heat within the boundary layer. When Re was large, viscous forces were minimal and hence the friction between the surface and the fluid was minimal which resulted to minimal dissipation of heat within the boundary layer.

(ii) When Kr was increased from 0.5 to 1, from curve-iii we noted that the heat dissipated in the boundary layer increased from 0.579673 K to 1.109492 K.

This was because when the curvature was increased, there was increased velocity gradient, the increased velocity gradient led to increased shear stresses. These shear stresses brought about friction between the fluid and the surface and in turn this friction force led to dissipation of heat within the boundary layer region represented by the formula

$$\tau = \mu \frac{\partial u}{\partial y}, \text{ which implies that when the velocity gradient increases it leads}$$

to an increase in the shear stress and in turn increased dissipation of heat.

From figure 3 we note that:-

(i) When Ec was increased from 1 to 10, from curve-iii we noted that the free stream velocity increased from 2.504238662 m/s to 2.504238663 m/s.

This was because when Ec was large; it implied that the kinetic energy dominated the boundary layer enthalpy which meant that the particles or molecules of the fluid had high velocities. When the Ec number was small, it implied that the kinetic energy was small and hence the particles had low velocities, hence when Ec was increased, the velocity also increased.

(ii) When Pe was increased from the 2 to 20, from curve-ii we noted that, the free stream velocity increased from 2.504200941 m/s to 2.504201 m/s.

This was because for large Pe it meant that rate of advection of the fluid dominated the flow rate of diffusion of the same quantity driven by an appropriate gradient, hence the fluid particles had high velocities which led to higher velocities.

From figure 4 we note that:

(i) When  $Ec$  was increased from 1 to 10, from curve-ii we noted that, the heat dissipated increased from 0.576463 K to 5.757413 K.

This was because for large  $Ec$ , it implied that the kinetic energy was large and hence the velocities were higher also when these particles increased in velocities, the vibrations also increased and this led to increased collision of the particles. These increased collisions of particles brought about dissipation of heat in the boundary layer region.

(ii) When  $Pe$  was increased from 2 to 20, from curve-iii we noted that, the heat dissipated in the boundary layer increased from 0.576463 K to 0.995561 K.

This was because large  $Pe$  led to increased velocities, this increased velocities of the fluid particles led to increased collision which in turn led to increased dissipation of heat.

### 3.1 Data Representation

The following data representation was obtained after the solving the equations governing the fluid flow.

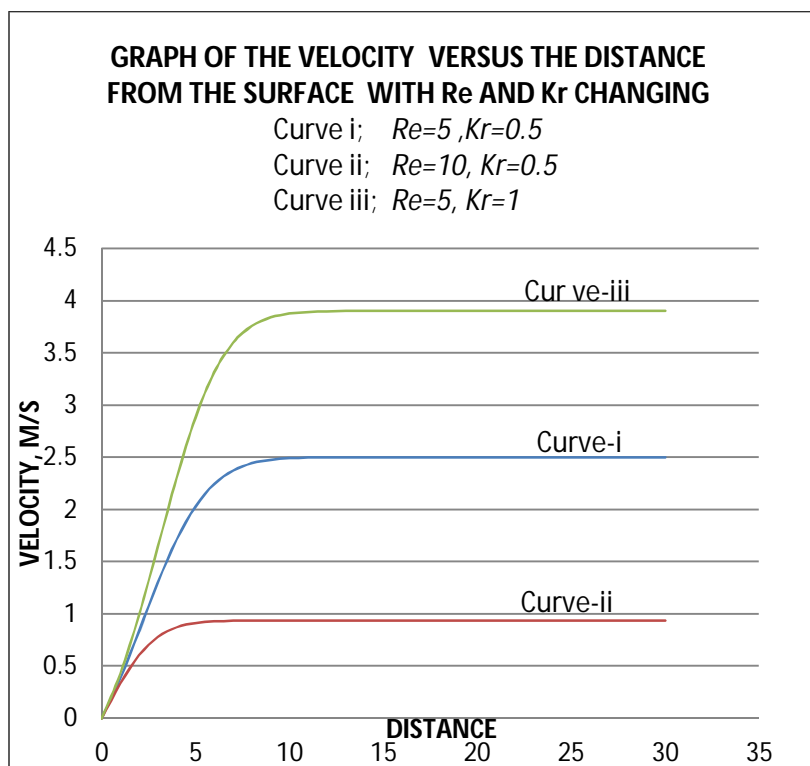


Figure 1: Velocity profiles for- $Ec=1$   $Pe=2$   $V=0.5$   $A=1$   $L=0.1$   $P_t=1$

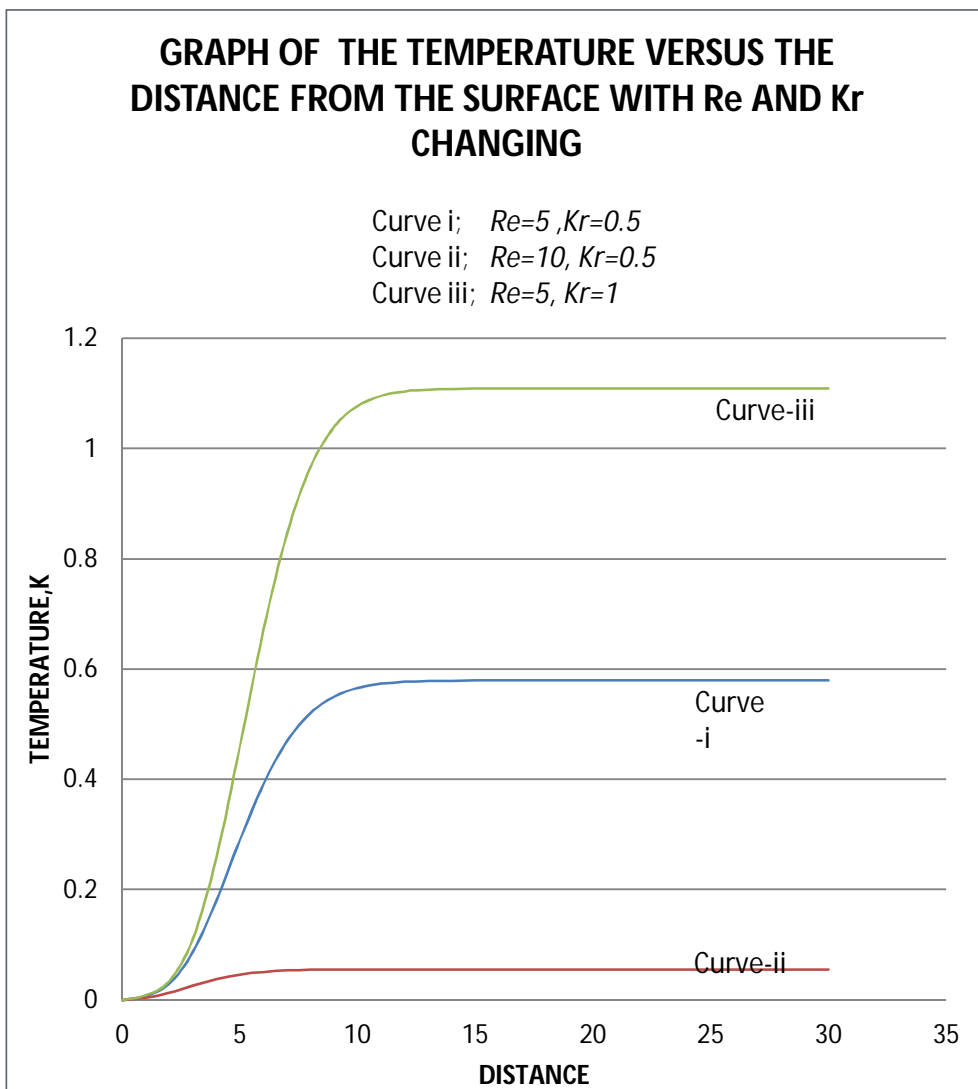


Figure 2: Temperature profiles for- $Ec=1$   $Pe=2$   $V=0.5$   $A=1$   $L=0.1$   $P_t=1$

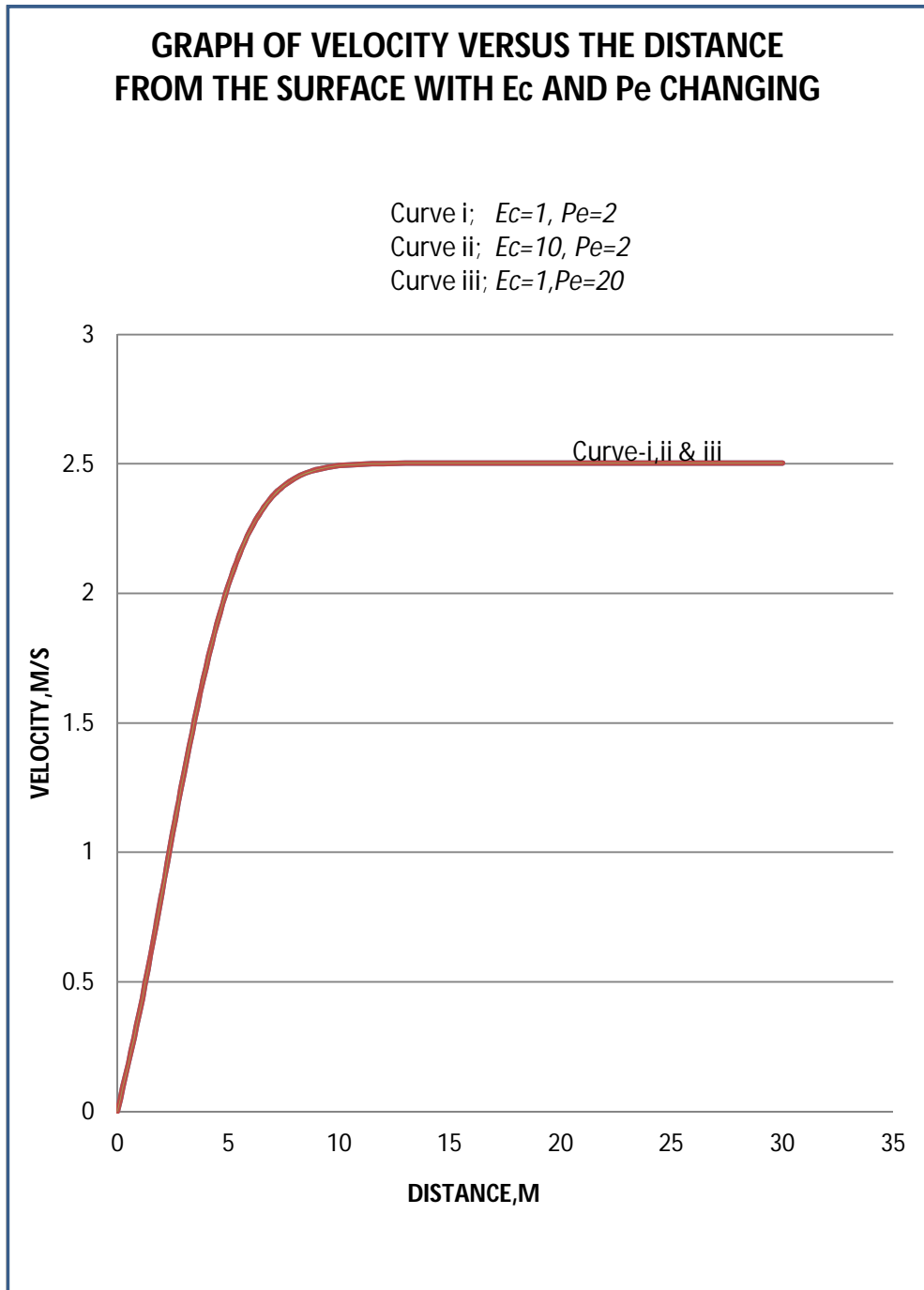


Figure 3: Velocity profiles for-  $Re=5$   $Kr=0.5$   $Pt=1$   $L=0.1$   $A=1$   $V=0.5$

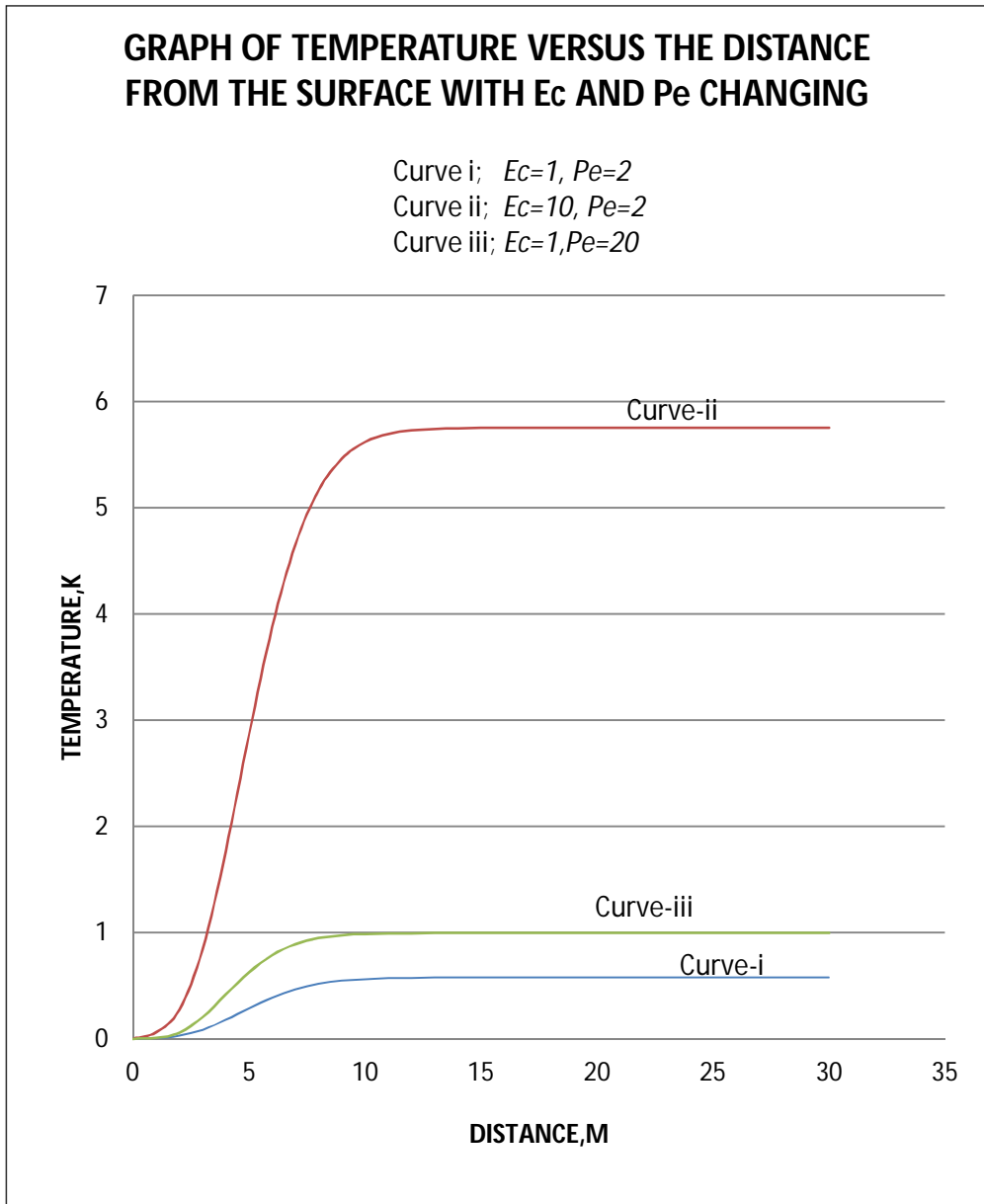


Figure 4: Temperature profiles for-  $Re=5$   $Kr=0.5$   $Pt=1$   $L=0.1$   $A=1$   $V=0.5$

#### 4.0 Conclusion

For a fluid flow over an axi-symmetrical body with curved surfaces, it was observed that when Reynolds number,  $Re$  was varied, that is the ratio of the inertia forces to the viscous forces say when  $Re$  was increased, the boundary layer thickness decreased and inertia forces dominated the viscous forces. When  $Re$  was decreased, the boundary layer thickness increased and inertia forces decreased. This matched the theoretical explanation since for increased  $Re$ , the viscous forces reduce and the boundary layer thickness reduces and this in turn reduces the dissipation of heat within the boundary layer. Hence when  $Re$  was increased, the boundary layer thickness reduced, velocity reduced and the temperature also reduced and when  $Re$  was reduced, the boundary layer thickness increased and the temperature also increased. Hence for a fluid flow over an axi-symmetrical surface with curved surfaces Reynolds number,  $Re$  is inversely proportional to the boundary layer thickness and both the velocity and the temperature.

When curvature of the surface was varied, this led to change in the velocity and also the temperature. When the curvature of the surface was increased, this led to increased velocity and increased temperature. When the curvature of the surface was decreased, this led to decreased velocity and temperature. Hence for a fluid flowing over an axi-symmetrical body with curved surfaces, the curvature was directly proportional to the temperature and the velocity.

When Eckert number was varied this also led to variation in both the temperature and the velocity. When Eckert number was increased, this led to increased velocity and also increased temperature. When Eckert number was decreased, this led to decreased velocity and also decreased temperature. Hence for a fluid flow over an axi-symmetrical surface with curved surfaces, Eckert number was directly proportional to both the velocity and the temperature.

When Peclet number,  $Pe$  was varied this also led to variation in both the temperature and the velocity. When  $Pe$  number was increased, this led to increased velocity and also increased temperature. When  $Pe$  number was decreased, this led to decreased velocity and also decreased temperature. Hence for a fluid flow over an axi-symmetrical surface with curved surfaces,  $Pe$  number is directly proportional to both the velocity and the temperature.

Reynolds number  $Re$ , affects both lift and drag in that when  $Re$  was increased, it led to decreased drag and when  $Re$  was decreased, it led to increased drag hence inverse proportionality. When  $Re$  is increased, this leads to increased lift and when  $Re$  is decreased, it leads to decreased lift hence direct proportionality.

**References**

Barenblatt G. I., Chorin A. J. and Protokishin V. M.(2002): A model of a turbulent boundary layer with a non-zero pressure gradient, Proceedings of National Academy of Science USA 2002, pp 5772-5776

Bouzidi M., Firdaouss Ms., Lallermannand P.(2001). Momentum transfer of a lattice Boltzmann fluid with boundaries. *Physics of Fluids*, **13**, 3452-9 OGT-268

Gordon C. Everstine(2010). Numerical solutions of partial differential equations by Gaithersburg, Maryland

Filipova O., Hanel D., (1998): Grid refinement for Lattice –BG-K models. *Journal of computational Physics*, **147**, pp 219-228, **158**, pp 139-160

Fukagata K., Iwamoto K., and Kasagi N. (2002). Contribution of the Reynold's stress distribution to the skin friction in wall bounded flows, *Journal of Physics of fluids*, **14**, pp 73-76

Khoshevis A. B and Saeed H.(2007). Calculation of turbulence intensities and shear stresses on concave surfaces by extending the low Reynolds turbulence model for curved walls, *international Journal of Dynamics of fluids*, **3**, pp 211-234

Mayle R. E., Blair M. F and Kopper F. G. (1979), Turbulent boundary layer heat transfer on curved surfaces, *American Society of Mechanical Engineers Journal of Heat transfer*, **101**, pp 521-523.

Mei R., Luo L. S, Shyy W. (1999). An accurate curved boundary treatment in lattice Boltzmann method, *Journal of Computational Physics*, **155**, pp 30-37

P. Bradshaw (2006). The analogy between streamline curvature and buoyancy in turbulent shearflow, *Journal of Fluid Mechanics*, **36**, pp 177-191

Prandtl L., (1904); Third International Mathematics Congress in Germany; Proceedings of congressional meeting, August 8, Heidelberg, Germany, pp 42-48.